Green Chemistry

PAPER

View Article Online
View Journal

Published on 05 April 2017. Downloaded by University of Tennessee at Knoxville on 05/04/2017 19:53:36.

Check for updates

Cite this: DOI: 10.1039/c6gc03627a

Effects of organosolv and ammonia pretreatments on lignin properties and its inhibition for enzymatic hydrolysis

Chang Geun Yoo,[a,b] Mi Li,[a,b] Xianzhi Meng,[c] Yunqiao Pu *[a] and Arthur J. Ragauskas *[a,b,c]

Lignin offers structural support and protection for plant cell walls; however, it also contributes to biomass recalcitrance and the costs of biofuel production *via* the biological pathway. Organosolv and ammonia pretreatments have been developed to reduce biomass recalcitrance and improve sugar release performance during enzymatic hydrolysis. It is believed that lignin properties are related to its inhibition on enzymatic hydrolysis; therefore, understanding the characteristics of lignin is a key for effective biomass conversion to biofuels. In this study, an organosolv pretreatment using 60% ethanol with 1.25% H_2SO_4 significantly deconstructed poplar lignin and reduced its molecular weights due to the cleavage of lignin inter-unit linkages. The organosolv pretreatment increased the contents of phenolic OH units and the lignin residue showed a high cellulase maximum adsorption capacity. Ammonia pretreatment with 5% ammonium hydroxide was not as effective as organosolv pretreatment on lignin deconstruction. Organosolv lignin residue had lower lignin S/G ratio than the untreated one. Compared to the organosolv lignin residue and untreated lignin, ammonia lignin residue had a higher cellulase adsorption affinity. In addition, the effects of lignin on cellulose hydrolysis was investigated and the results suggested that the presence of lignin with cellulose substrates reduced cellulose hydrolysis, and its inhibitory effect was primarily determined by the lignin properties after each pretreatment. The organosolv pretreatment resulted in a slightly lower cellulase binding strength (249.7 mL g^{-1}) on poplar lignin than that on untreated samples (261.1 mL g^{-1}), while ammonia lignin residue showed a higher cellulase binding strength (402.8 mL g^{-1}) and had more significant inhibition effect on cellulose hydrolysis. These results demonstrated that the binding strength significantly affected the lignin-derived inhibition on enzymatic hydrolysis of cellulose in the cellulose-lignin mixtures.

Received 31st December 2016,
Accepted 27th March 2017

DOI: 10.1039/c6gc03627a

rsc.li/greenchem

Introduction

Lignocellulosic biomass is a promising feedstock for alternative fuels and chemicals due to its abundance, high sugar content, and low feedstock price. In addition, utilization of biomass can contribute to reduce greenhouse gas emission by replacing current petroleum-based products; therefore, biomass conversion strategies have been considered as a "green" approach.[1] To achieve efficient biomass utilization, it is necessary to overcome biomass recalcitrance which is caused by cellulose crystallinity, physical barriers associated with lignin and/or hemicellulose, non-productive enzyme binding onto lignin, and other considerations. Among many biomass recalcitrance factors, lignin poses a crucial challenge in the biological conversion process for biofuels and biomaterials. Lignin is a heterogeneous aromatic polymer derived from phenolic monomers such as *p*-coumaryl alcohol, coniferyl alcohol, and sinapyl alcohol with complex inter-unit linkages such as β-*O*-4, β–β, β-5, 5–5, and 4-*O*-5 structural motifs. Lignin-derived inhibition has been proposed to occur in four ways: (1) blocking the surface of carbohydrates as a physical barrier; (2) forming lignin-carbohydrate complexes (LCC); (3) binding to enzymes non-productively; (4) deactivating enzymes with soluble lignin fragments.[2,3] Lignin forms a highly cross-linked matrix of aromatics and fills the space between cellulose, hemicellulose and pectin in plant cell walls, with its physical structure inhibiting enzyme access to cellulose by surrounding cellulose fiber.[4,5] The inhibitory effect of LCC lin-

[a]*BioEnergy Science Center and Biosciences Division, Oak Ridge National Laboratory, Oak Ridge, TN 37831, USA. E-mail: puy1@ornl.gov, aragausk@utk.edu*
[b]*UT-ORNL Joint Institute for Biological Science, Oak Ridge National Laboratory, Oak Ridge, TN 37831, USA*
[c]*Department of Chemical and Biomolecular Engineering & Center for Renewable Carbon, Department of Forestry, Wildlife, and Fisheries, University of Tennessee, Knoxville, TN 37996, USA*

Published on 05 April 2017. Downloaded by University of Tennessee at Knoxville on 05/04/2017 19:53:36.

kages on enzymatic hydrolysis was also reported in previous studies.[2,6] Non-productive enzyme binding onto lignin occurs through hydrophobic, electrostatic, and/or hydrogen-bonding interactions.[7–9] For example, Yang and Pan discussed the lignin inhibition effects by hydrophobicity and phenolic hydroxyl group in lignin.[7] Nakagame *et al.* also showed cellulase adsorption on lignin occurred by hydrophobic and electrostatic interactions.[8] Similarly, Sun and his co-workers indicated undesirable enzyme binding on lignin by combination of hydrogen bonding and hydrophobic interaction.[9] In addition, soluble lignin (*i.e.*, degraded lignin fragments) is usually generated by decomposition of lignin during pretreatment leading to the subsequent enzyme deactivation. Ximenes *et al.* reported the inhibition and deactivation effects of lignin on enzymatic hydrolysis of cellulose by phenolic compounds formed by lignin degradation.[10] Therefore, further studies are needed to either develop new enzymes with high resistance to the phenolics or include additional steps to remove the undesirable compounds before enzymatic hydrolysis to combat these effects.

Pretreatment is a step that aims to remove and/or reduce the biomass recalcitrance to improve enzymatic hydrolysis. Pretreatment methods have been developed using different solvents/catalysts such as acids, alkali, organic solvents, and ionic liquids.[11–18] Among many pretreatments, organosolv and ammonia pretreatments have been reported as effective lignin-targeting methods for overcoming biomass recalcitrance resulting in either lignin removal or modification. Organosolv pretreatment significantly removes and modifies lignin using an organic solvent such as ethanol, acetone, or methanol with an acid or base catalysts.[19,20] Recently, applicable solvents in organosolv pretreatments were expanded to methyl isobutyl ketone, 2-methyltetrahydrofuran, tetrahydrofuran, γ-valerolactone, and others.[18,21–27] Ionic liquids consisting of organic cations and anions like cholinium-amino acid ionic liquids were also applied for fractionation and delignification of biomass.[21] The ammonia pretreatment is another method that is commonly used with herbaceous biomass.[28,29] Ammonia pretreatment has been reported to enhance the enzymatic digestibility of cellulose and hemicellulose fractions with alteration of some lignin properties and/or partial lignin removal.[13,30] While the degree of delignification (*i.e.*, lignin removal) of biomass varies depending on the pretreatment methods employed, it is difficult to completely remove lignin without the risk of carbohydrate loss and excessive chemical and energy consumption. The lignin residues, which usually remain in biomass after pretreatment, still affect the ensuing enzymatic hydrolysis. Therefore, understanding the structural changes on lignin residues can be insightful for the further improvement of biomass conversion.

Inhibitory effects of several natural/technical lignins have been investigated.[2,7–9,31–33] However, most of previous studies either tested with soluble lignin fractions in pretreatment solvents or conducted lignin isolation steps after pretreatments. For instance, Yang and Pan studied with organosolv lignins, but these lignins were recovered from soluble fractions in the pretreatment solvents.[7] Sun *et al.* studied with pretreated lignin, but only tested with hydrothermal pretreated aspen.[9] Li *et al*. isolated lignins through a two-step sulfuric acid hydrolysis, which can cause the modification of lignin properties.[33] So far, the property changes and effects of insoluble lignin residues after organosolv and ammonia pretreatments on enzyme performance were not fully understood yet. Here, lignin isolated from poplar was used as a substrate to investigate the changes on physicochemical properties of poplar lignin by two different lignin-targeting pretreatments (*i.e.*, organosolv and ammonia pretreatment). Cellulolytic enzyme lignin (CEL) was used as a feedstock in this study. Compared to the traditional milled wood lignin (MWL), CEL shows higher isolation yield and is widely used as a representative of lignin in biomass with minimal structural alternations.[34,35] The structural changes on poplar lignin were observed by analyzing the lignin properties including molecular weight, structural information, hydroxyl group contents and compositions. The effects of pretreated lignin residues on the enzymatic hydrolysis of cellulose were also evaluated by measuring enzyme adsorption and enzymatic digestibility. The relationship between lignin properties and its inhibition effects investigated in this study can help determine pretreatment methods and reaction conditions for efficient biomass conversion.

Results and discussion

Deconstruction of lignin by organosolv and ammonia pretreatments

Lignin deconstruction has been observed in many pretreatment studies including organosolv and ammonia pretreatments.[20,28] During the pretreatments, lignin was decomposed and solubilized by the pretreatment solvents which removed a proportion of lignin from the pretreated solids. Lignin solubilization was calculated by measuring the masses of the soluble and insoluble fractions after each pretreatment. Table 1 presents the lignin solubilization data after each pretreatment. A fraction of cellulolytic enzyme lignin (CEL) was solubilized by both organosolv and liquid ammonia pretreatments. In particular, the organosolv pretreatment showed potent effects on lignin solubilization (74%), while ammonia pretreatment resulted in much less lignin solubilization (~29%). Compared with CEL, Table 1 also shows that the purity of lignin in the solid residues slightly increased to 95–97% after both pretreatments.

Molecular weight is another index to evaluate the physical properties of lignin. For a deeper understanding of lignin

Table 1 Solubilization and chemical composition of lignin residues after organosolv and ammonia pretreatment

Lignin	Solubilization [wt%]	Lignin [wt%]	Glucan [wt%]	Xylan [wt%]
CEL	—	89.7 ± 0.9	5.2 ± 1.1	3.7 ± 0.6
AR	29.3 ± 1.0	94.7 ± 0.5	2.9 ± 0.4	0.8 ± 0.1
OR	74.3 ± 1.5	96.8 ± 0.5	3.0 ± 0.5	0.0 ± 0.0

This journal is © The Royal Society of Chemistry 2017

Published on 05 April 2017. Downloaded by University of Tennessee at Knoxville on 05/04/2017 19:53:36.

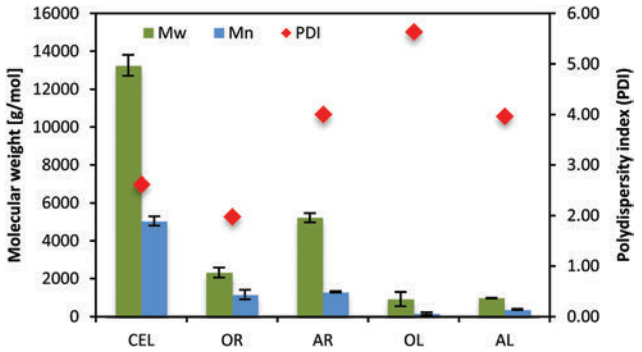

Fig. 1 Molecular weights and polydispersity index of the untreated and organosolv and ammonia pretreated lignin residues.

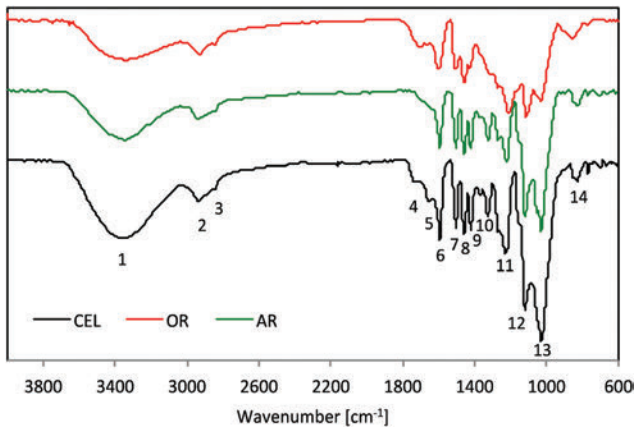

Fig. 2 FTIR spectra from the untreated and organosolv and ammonia pretreated lignin residues.

deconstruction, the molecular weights of lignin fractions after organosolv and ammonia pretreatments were analyzed by gel permeation chromatography (GPC). Fig. 1 presents the weight average molecular weight (M_w), number average molecular weight (M_n), and polydispersity index (PDI, M_w/M_n) of soluble and insoluble lignin fractions after each pretreatment. As Fig. 1 shows, M_w and M_n of cellulolytic enzyme lignin (CEL), which was isolated from poplar, were significantly reduced by both pretreatments. The organosolv lignin residue (OR) was ~2300 g mol^{-1} and ~1200 g mol^{-1} for M_w and M_n, and ammonia lignin residue (AR) had ~5200 and ~1300 g mol^{-1} of M_w and M_n, respectively. Soluble fraction in each pretreatment (organosolv lignin (OL) and ammonia lignin (AL)) had similar M_w and M_n, even though organosolv pretreatment dissolved more lignin than the ammonia pretreatment. In order to understand the molecular weight distribution of lignins, the PDI of each sample was compared. OR showed a lower PDI (1.98), while OL had a higher PDI (5.64) compared to that of CEL (2.63). This indicated that the lignin residues after organosolv pretreatment became more uniform in terms of molecular weight. On the other hand, ammonia pretreatment showed different results; the PDIs of both AR (4.01) and AL (3.97) were higher than that of CEL. The results suggested that ammonia pretreatment led to relatively broader molecular weight distributions in both soluble lignin and solid residues. Overall, organosolv pretreatment resulted in more significant solubilization and decrease of the molecular weight compared to the effects of ammonia pretreatment on lignin molecular weight. These differences in lignin solubilization and the molecular weight changes by organosolv and ammonia pretreatments imply that the delignification mechanisms of each pretreatment could be different.

Changes on physicochemical properties of lignin by organosolv and ammonia pretreatments

Although lignin depolymerization is one of the major pretreatment effects, it is not sufficient to explain all the changes in biomass recalcitrance associated with lignin structures by these pretreatments. The chemical fingerprint of untreated lignin (CEL) and pretreated lignin residues (OR and AR) was analyzed by measuring the adsorption and transmission of functional groups including hydroxyl (O–H), alkene (C=C), ester (–COO–), aromatics (Ar), ketone (C=O), ether (C–O–C) and others using FTIR (Fig. 2 and Table 2). Lower peaks corresponding to the hydroxyl group, assigned at 3388 cm^{-1}, were observed in the pretreated lignin residues (OR and AR) compared to CEL (#1 in Fig. 2 and Table 2). The results indicated that the total hydroxyl groups including aliphatic and aromatic OH in the lignin decreased by both pretreatments. The C–H stretching peaks in OR and AR at 2952 and 2876 cm^{-1} (#2 and 3 in Fig. 2 and Table 2) were also smaller than the peak in CEL. These peaks represented the C–H bonds in methyl and methylene groups. The C=O stretching peak corresponding unconjugated carbonyl group at 1741 cm^{-1} (#4 in Fig. 2 and Table 2) was lower in AR, while the peak in OR was similar to the one in CEL. The peak near 1670 cm^{-1}, which represents C=O in lignin side chains conjugated with aromatics also decreased in the pretreated lignin residues (#5 in Fig. 2 and Table 2). This change could be attributed to the removal of

Table 2 Relative peak intensity of FTIR spectra from the untreated and organosolv and ammonia pretreated lignin residues

		Relative peak intensity		
#	Wavelength [cm^{-1}]	CEL	OR	AR
1	3388	1.00	0.88	0.90
2	2952	1.00	0.98	0.96
3	2876	1.00	0.97	0.97
4	1741	1.00	1.00	0.94
5	1670	1.00	0.98	0.95
6	1595	1.00	0.90	0.93
7	1507	1.00	0.94	0.97
8	1464	1.00	0.97	0.97
9	1453	1.00	0.98	0.97
10	1327	1.00	0.99	0.98
11	1221	1.00	0.98	0.92
12	1120	1.00	0.77	0.90
13	1033	1.00	0.62	0.80
14	847	1.00	1.01	0.99

Published on 05 April 2017. Downloaded by University of Tennessee at Knoxville on 05/04/2017 19:53:36.

p-hydroxybenzoate (PB) and/or formation of oxidized lignin subunits during the pretreatments. The peaks for aromatic ring stretching and vibrations occurred at 1595 and 1507 cm^{-1} (#6 and 7 in Fig. 2 and Table 2), and the peaks for C–H deformation at 1464 and 1424 cm^{-1} (#8 and 9 in Fig. 2 and Table 2) decreased by both pretreatments. In particular, the organosolv pretreatment notably reduced these peaks. The peaks for C–O vibration of syringyl (S) and guaiacyl (G) rings were assigned at 1327 and 1221 cm^{-1} (#10 and 11 in Fig. 2 and Table 2), respectively. The estimated S and G peaks indicated that the ammonia pretreatment reduced the G unit content in the lignin. A decrease in cellulose contaminants by these pretreatments was observed at 1120 cm^{-1} (#12 in Fig. 2 and Table 2), which represents carbon ring stretching in cellulose. This data confirms the enhanced lignin purity in the compositional analysis results (Table 1). The C–O–C stretching peak at 1033 cm^{-1} (#13 in Fig. 2 and Table 2) also decreased in the pretreated residues, while no significant change was monitored on the peak of aromatic C–H deformation out of plane at 847 cm^{-1} (#14 in Fig. 2 and Table 2).

In Fig. 3 and 4, 2D ^{1}H–^{13}C HSQC NMR spectra profiled the structural changes of lignin after the organosolv and ammonia pretreatments. In the aliphatic regions of the HSQC NMR spectra (Fig. 3), β-*O*-4, β-5, and β–β were the dominant inter-unit linkages in poplar CEL. The peaks at δ_C/δ_H 71.4/4.81 ppm, δ_C/δ_H 86.9/5.47 ppm, and δ_C/δ_H 85.1/4.65 ppm were ascribed to the correlation of α position of β-aryl ether (β-*O*-4), phenylcoumaran (β-5), and resinols (β–β), respectively, and used for estimation of inter-unit linkages. A peak representing β–β linkage was clearly detected and the rest peaks appeared at the noise level in OR, while the peaks for these major inter-unit linkages were remained to be observed in AR, suggesting more significant deconstruction of lignin after organosolv pretreatment. This might partially explain the remarkable reduction of molecular weights of OR compared to that of AR in Fig. 1.

Aromatic compositions in each lignin were presented in Fig. 4. The poplar lignin demonstrated its major aromatic compositions consisting of S and G units along with considerable amounts of PB. The quantification of each compositional unit was conducted with the volume integration of peaks of $S_{2/6}$, α-oxidized $S_{2/6}$, G_2, and $PB_{2/6}$ observed at δ_C/δ_H 104.0/6.68 ppm, δ_C/δ_H 106.3/7.27 ppm, δ_C/δ_H 111.0/6.96 ppm, and δ_C/δ_H 131.3/7.64 ppm, respectively. The peaks for lignin subunits such as S and G units were significantly reduced in intensity and shifted in its chemical shifts in OR compared to these peaks in CEL (Fig. 4). It indicated that the organosolv pretreatment did not only deconstruct, but it also modified the lignin structures. In particular, the peaks of condensed $S_{2/6}$ and G_2 were observed at δ_C/δ_H 105.3/6.37 ppm and δ_C/δ_H 112.4/6.74 ppm, respectively. The aromatic region of AR did not show notable changes except a slight decrease in the peak of the G unit. Besides the lignin subunits, the peaks of PB in OR and AR were reduced when compared with CEL.

Table 3 summarizes the quantitative information of lignin subunits and inter-unit linkages in each lignin sample for the HSQC NMR analysis results. The S/G ratio in the CEL (1.50) decreased to 1.33 after organosolv pretreatment, while it increased to 2.84 after ammonia pretreatment. Based on the S and G unit contents in the lignin residues, organosolv pretreatment showed a decreased S/G ratio, while ammonia pretreat-

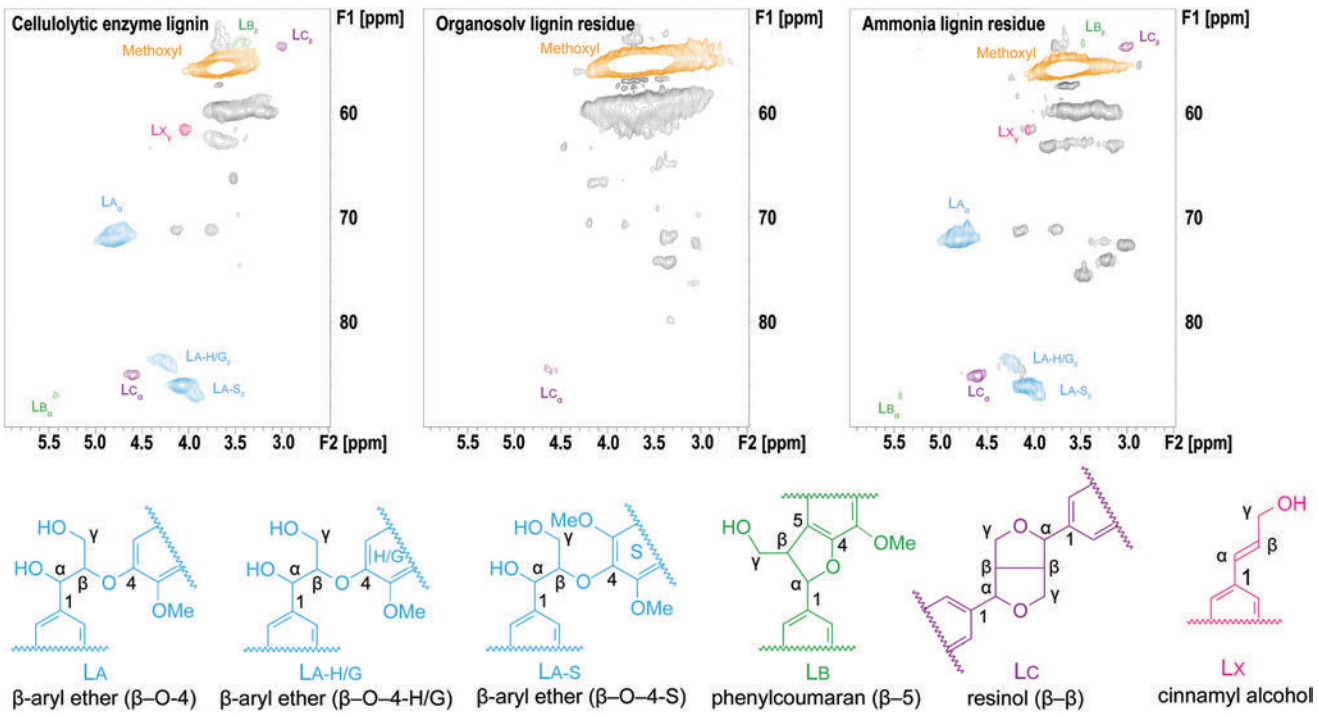

Fig. 3 Aliphatic regions of 2D HSQC NMR spectra from the untreated and organosolv and ammonia pretreated lignin residues.

This journal is © The Royal Society of Chemistry 2017

Published on 05 April 2017. Downloaded by University of Tennessee at Knoxville on 05/04/2017 19:53:36.

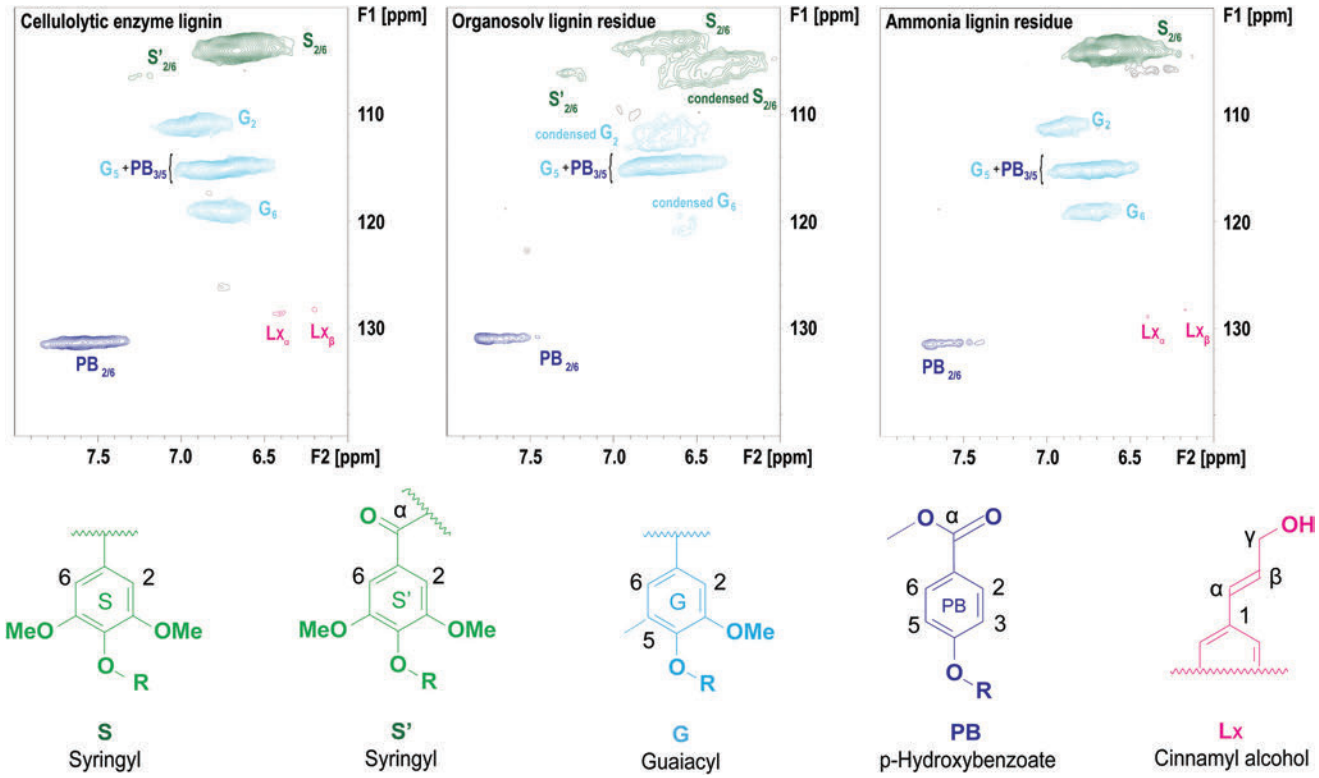

Fig. 4 Aromatic regions of 2D HSQC NMR spectra from the untreated and organosolv and ammonia pretreated lignin residues.

Table 3 Quantitative information for lignin subunits and inter-unit linkages in the untreated and organosolv and ammonia pretreated lignin residues

	CEL		OR		AR		OL		AL	
	Ar%[a]	%[b]	Ar%[a]	%[b]	Ar%[a]	%[b]	Ar%[a]	%[b]	Ar%[a]	%[b]
Lignin subunits										
Syringyl (S)	60		57		74		63		75	
Guaiacyl (G)	40		43		26		37		16	
S/G	1.50		1.33		2.84		1.72		4.73	
Hydroxycinnamates										
p-Hydroxybenzoate (PB)	16		7		6		3		24	
Inter-unit linkages										
β-*O*-4	54	89	0.9	35	46	89	1.4	42	29	82
β-5	2.6	4	0.3	13	1.5	3	1.1	32	1.9	5
β–β	4.3	7	1.3	52	4.3	8	0.8	25	4.6	13

[a] Content (%) expressed as a fraction of S + G + H. [b] Content (%) expressed as a fraction of β-*O*-4 + β-*5* + β–β.

ment reduced more G unit than S unit from the lignin. Another notable change was the decrease in the PB content over total lignin subunits. After the pretreatments, both OR and AR had lower PB contents (7 and 6%, respectively) than CEL had (16%). From these results, solubilization of PB into the pretreatment solvents is anticipated. PB exists as free-phenolic pendant units on lignin and exclusively attaches at the γ-position of lignin side-chains.[36] The relatively high PB content in AL (24%) indicated the solubilization of PB by the ammonia pretreatment. On the contrary, the presence of less remaining PB in the OR and OL showed further decomposition and/or transformation of PB during the organosolv pretreatment. HSQC NMR analysis also revealed the evidence of lignin deconstruction in aliphatic regions (Fig. 3 and Table 3). The evidence for the cleavage of inter-unit linkages by organosolv pretreatment was observed in both OR and OL. The content of total lignin inter-unit linkages including β-*O*-4, β–β, and β-5 linkages over total lignin aromatic subunits (Ar%) in OR was only 2.5%, while CEL had 61%. Significant reductions in β-*O*-4 and β-5 linkages took place in OR, thus about 52% of inter-unit linkages in OR was β–β linkages. In OL, lignin inter-unit linkages were observed at the noise level and the amounts

Published on 05 April 2017. Downloaded by University of Tennessee at Knoxville on 05/04/2017 19:53:36.

were only 3.3% over total lignin aromatic subunits. The reduced lignin inter-unit linkages explain the cleavages of lignin linkages by the organosolv pretreatment. The dramatic reduction of β-*O*-4 linkages in OR and OL indicates effectiveness of organosolv pretreatment on the breakage of β-aryl ether linkages. In AR, the content of the total lignin inter-unit linkages over total aromatic regions (Ar%) was slightly reduced (52.1%). The ammonia pretreatment decreased the contents of β-*O*-4 and β-5 linkages, but the changes on inter-unit linkages were minimal. In AL, the β-*O*-4, β-5, and β–β linkages were 29%, 1.9%, and 4.6%, respectively. Easier cleavage on β-*O*-4 linkages than other C–C linkages was revealed from the results.

Hydroxyl groups of lignin are important characteristics associated with the physicochemical properties of lignin. ^{31}P NMR analysis was conducted by quantifying different types of hydroxyl (OH) groups on lignins, as shown in Scheme 1. The content of each OH group was measured by observing the phosphorylated hydroxyl groups. Fig. 5 shows the quantitative ^{31}P NMR analysis results with CEL, OR, and AR. The total content of OH group in CEL (6.17 mmol g^{-1}) decreased to 5.73 and 5.06 mmol g^{-1} for OR and AR, respectively. Specifically, the aliphatic OH group was a dominant OH group in CEL (5.25 mmol g^{-1}), and it was reduced by the organosolv and ammonia pretreatments to 1.95 and 4.24 mmol g^{-1}, respectively. This result supports the HSQC NMR result indicating the cleavage of lignin inter-unit linkages in both pretreatments. The ammonia pretreatment increased C5 substituted OH content, mainly from syringyl unit, and decreased guaiacyl OH content and aliphatic OH content, and the results were consistent with the increased S/G ratio measured by HSQC NMR in Table 3. On the other hand, the relative content ratio of C5 substituted OH and guaiacyl OH (2.07) in OR was higher than the ratio in CEL (0.82). The results from HSQC and ^{31}P NMR could be different, since HSQC NMR measured the ratio of total S and G contents, while ^{31}P NMR only detected free phenolic OH in lignins. Also, Pu *et al.* reported that the signals from syringyl OH and C5 substituted guaiacyl OH were overlapped.[37] Lignin could be condensed under acid conditions

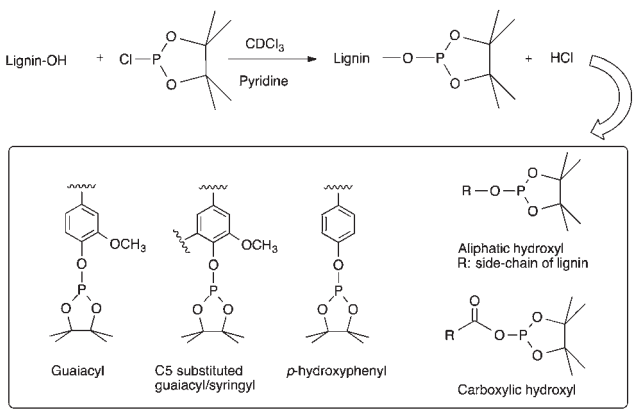

Scheme 1 Reaction scheme of phosphitylation of lignin hydroxyl groups with 2-chloro-4,4,5,5-tetramethyl-1,3,2-dioxaphospholane.

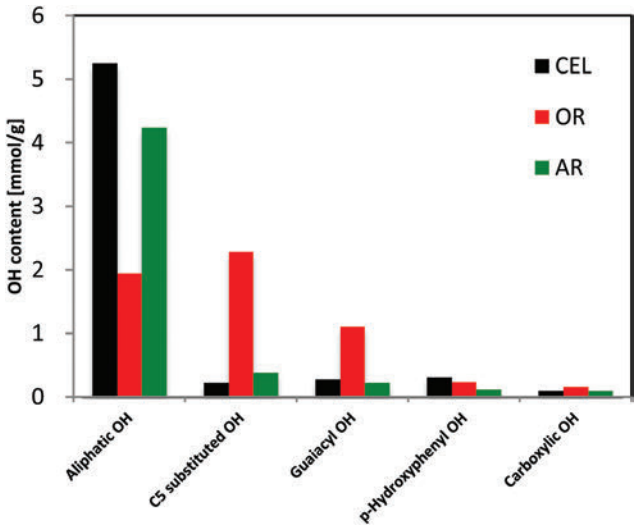

Fig. 5 Hydroxyl group content in the untreated and organosolv and ammonia pretreated lignin residues.

during the organosolv pretreatment;[38] therefore, it would be possible that organosolv pretreatment produced the C5-condensed G units, which were counted as the C5 substituted OH content. OR had a much higher phenolic OH content (3.62 mmol g^{-1}) than AR (0.72 mmol g^{-1}) and CEL (0.83 mmol g^{-1}). CEL was isolated from poplar, thus the observed *p*-hydroxyphenyl OH was mainly attributed from PB. The content of *p*-hydroxyphenyl OH decreased, while content of carboxylic OH was not significantly changed by the pretreatments.

These results demonstrated that the organosolv pretreatment deconstructed lignin by significant solubilization and decrease of the molecular weights. The reduced content of lignin inter-unit linkages over aromatics in HSQC NMR analysis represents the cleavage of lignin inter-unit linkages by the pretreatment. Decreases in the aliphatic OH content reported in ^{31}P NMR analysis results also point towards lignin decomposition. Relatively increased contents of the phenolic S and G units by cleavage of lignin and decreased PB content after organosolv pretreatment were observed in ^{31}P NMR analysis results. In addition, the HSQC spectra showed that the condensed S and G units were formed under the acidic conditions.

Ammonia pretreatment also decomposed poplar lignin; however, it was not as effective as organosolv pretreatment on the lignin deconstruction based on the solubilization and molecular weight. Cleavage of lignin inter-unit linkages was verified by both NMR analyses. In specific, HSQC NMR result indicated the cleavage of β-*O*-4 and β-5 linkages, although the changes were not significant. In spite of significant deconstruction of lignin, the ammonia pretreatment reduced more G unit than S unit from the lignin, thus the S/G ratio of both soluble and residual fractions were higher than that of the original lignin (CEL). The increase of S/G ratio was confirmed with decreased guaiacyl OH in the ^{31}P NMR results. Liquid ammonia pretreatment showed remarkable delignification and modification with agricultural residues and herbaceous plants,

 This journal is © The Royal Society of Chemistry 2017

Published on 05 April 2017. Downloaded by University of Tennessee at Knoxville on 05/04/2017 19:53:36.

but it was not effective on woody biomass.[39,40] In herbaceous plants, recalcitrance is believed to mainly come from ferulate cross-linking, and the ammonia treatment was showed to cause cleavage and/or transformation of ferulate. For instance, improved enzymatic hydrolysis of corn stover after ammonia pretreatment was mainly due to the cleavage of ferulate and conversion of ferulate and *p*-coumarate esters to amides and acids.[13] Lignin structure in poplar is different from that in the herbaceous plants; in other words, lignin-derived recalcitrance is probably caused by different reasons. Mild deconstruction and modification of lignin with poplar CEL can be explained by the lignin compositional and structural differences between species. It implies that the physical and chemical properties of lignin are key information for biomass utilization.

Impact of organosolv and ammonia pretreatments on lignin for cellulase adsorption and enzymatic digestibility of cellulose

Lignin-derived inhibitory effects on enzyme activity like non-productive enzyme adsorption to lignin have been discussed in many studies.[2,7–9,31,32,41–43] Among many studies, enzyme adsorption onto lignin is viewed as a potent inhibitor for biological conversion of biomass. Previous studies were conducted either with soluble lignin fractions, which are mostly washed out after the pretreatments, or with the isolated lignin from different species. In this study, organosolv and ammonia pretreated lignin residues, which are close to the lignin fraction retained in the pretreated biomass solids, were used for measuring the lignin-derived inhibitory effects. Adsorption parameters of cellulase on lignin residues after each pretreatment were calculated and compared. Fig. 6 compares Langmuir adsorption isotherms with the lignin residues after the organosolv and ammonia pretreatments. OR showed higher cellulase adsorption than other lignins (CEL and AR) and Avicel which was tested as a cellulose control. In specific, the maximum adsorption capacity (Γ_{max}) of OR (94.9 mg g^{-1}) was higher than CEL (65.3 mg g^{-1}), while Γ_{max} of AR (60.4 mg g^{-1}) was slightly lower (Table 4). The high adsorption capacity of OR can be explained by the deconstructed OR structure, which had more binding sites like phenol hydroxyl (syringyl OH, guaiacyl OH, and *p*-hydroxyphenyl OH) as presented in ^{31}P NMR analysis. Larger surface area and more retained aromatics were also anticipated in the OR based on its lower molecular weights, significant reduction of inter-unit linkages, and higher aromatic OH contents in the aforementioned lignin characteristics. Both surface area and content of aromatics in the lignin are correlated to the adsorption capacity,[7] thereby higher maximum adsorption capacity of OR is explainable. Interestingly, the adsorption affinity (K) and binding strength (R) of each lignin show opposite trends (Table 4). OR had the lowest affinity (2.6 mL mg^{-1}) and binding strength (249.7 mL g^{-1}) with cellulase, while AR had remarkably higher affinity (6.7 mL mg^{-1}) and binding strength (402.8 mL g^{-1}) than those values (K = 4.0, R = 261.1 mL g^{-1}) in CEL.

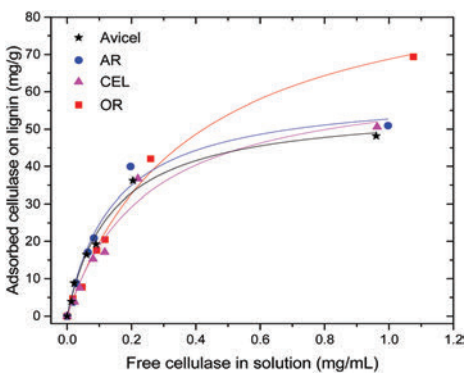

Fig. 6 Cellulase adsorption isotherm on the untreated and organosolv and ammonia pretreated lignin residues.

Table 4 Adsorption capacity, adsorption affinity, and binding strength from cellulase adsorption on the untreated and organosolv and ammonia pretreated lignin residues

	Γ_{max} (mg g^{-1})	K (mL mg^{-1})	R (mL g^{-1})
Avicel	56.2	7.1	401.7
AR	60.4	6.7	402.8
OR	94.9	2.6	249.7
CEL	65.3	4.0	261.1

Different physicochemical characteristics were observed in the lignin residues after organosolv and ammonia pretreatments. To evaluate the inhibition of each lignin residue on cellulose hydrolysis, the enzymatic hydrolysis of Avicel mixed with each lignin residue after organosolv and ammonia pretreatments was investigated. Fig. 7 presents the glucose yield of cellulose (Avicel) physically mixed with lignin residues. Two different lignin residue loadings (5 mg and 20 mg) were tested. Overall, the cellulose-lignin residue mixtures showed lower glucan digestibilities than the control (Avicel only) had. Addition of 5 mg lignin residue lowered 3–9% glucose yield at 72 h enzymatic hydrolysis (Fig. 7a). AR prevented the enzymatic hydrolysis most, and CEL and OR similarly lowered the glucose yields. The inhibitory effects by the lignin residues became larger when the loadings increased to 20 mg. At 72 h hydrolysis, the presence of 20 mg of OR and CEL reduced 9 and 13% of the glucan digestibility of Avicel in the mixtures, respectively (Fig. 7b). The inhibition effect of AR on cellulose hydrolysis was much more significant than other lignin mixtures had, thereby the glucan digestibility of Avicel-lignin mixture was 23% lower than that of the control. The results imply that the modification of lignin characteristics affects its inhibitory effects on enzymatic hydrolysis.

Both binding capacity and adsorption affinity of lignin to enzymes have been used as indices of enzyme adsorption to lignin in predicting its inhibitory effect.[7,9] Maximum adsorption capacity of lignin was also investigated to measure its inhibition on enzymatic hydrolysis.[7,31,41,43] A negative effect of the binding affinity of lignin on enzymatic hydrolysis of Avicel was reported.[9] Recently, overall non-productive adsorption was determined by accounting for both how much enzymes and how strongly they bind on lignins.[9] Therefore, binding

Published on 05 April 2017. Downloaded by University of Tennessee at Knoxville on 05/04/2017 19:53:36.

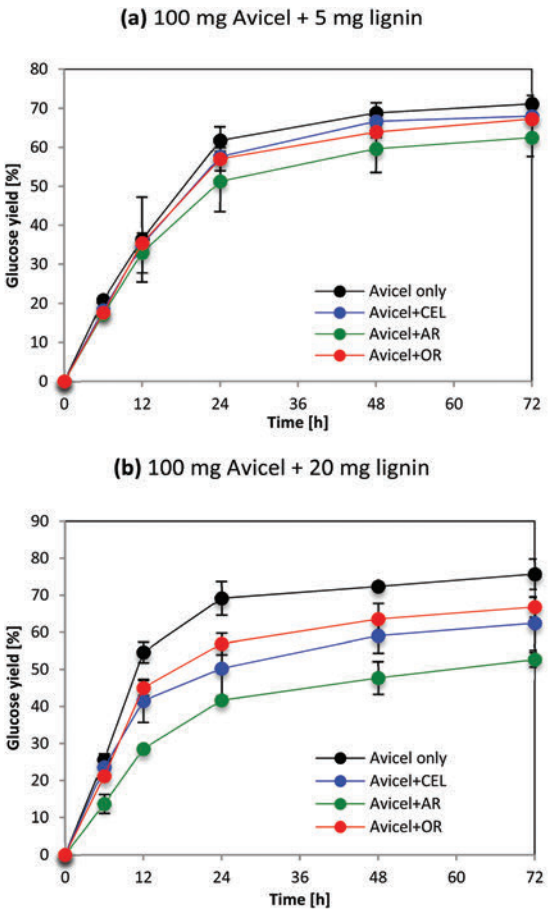

Fig. 7 Effect of the lignin residues on enzymatic hydrolysis of Avicel.

strength was introduced to estimate the amounts of enzymes onto lignins by incorporating these two factors. In particular, maximum adsorption capacity and adsorption affinity were conflicted in the enzyme adsorption test, thus the binding strength representing both factors together is a proper indicator for the overall inhibitory. The binding strength was positively correlated to the affinity. It implies that the binding strength of lignin residue was mainly driven by adsorption affinity of lignin. However, the driving factor for binding strength can be changed depending on the biomass species and/or processing conditions; thereby it needs to consider both the maximum capacity and affinity for better estimation.

In this study, AR had the higher lignin S/G ratio and binding strength, while it caused lower glucan digestibility than CEL resulted. On the contrary, OR showed lower lignin S/G ratio, adsorption affinity, and binding strength with the similar or higher glucan digestibility than CEL had. As a result of the decreases of non-productive enzyme adsorption parameters, the glucan digestibility of Avicel in the mixture increased, which means, low lignin S/G ratio might play a role in alleviating the lignin-derived inhibition on enzymatic hydrolysis. Guo *et al.* reported that lower lignin S/G ratio had a higher enzyme adsorption.[31] However, they also mentioned that the S/G ratio affects lignin cross-linking and enzyme accessibility. For this reason, in spite low lignin S/G ratio of OR resulted in high adsorption capacity of lignin, high glucose yield could be achieved. Transgenic poplar with high syringyl content showed improved resistance to degradation.[44] Qin and co-workers also reported the inhibition effect by methoxy group in phenolics on enzyme activity.[45] These intriguing results point out that lignin-derived inhibition can be determined and changed by multiple lignin properties depending on the species and process conditions.

Conclusions

The organosolv and ammonia pretreatments are lignin-targeting pretreatment methods to alleviate the biomass recalcitrance for biofuels production. Organosolv pretreatment resulted in a significant deconstruction of lignin by cleavage of inter-unit linkages and condensation of S and G units; thereby these changes on lignin properties increased the maximum adsorption capacity. Ammonia pretreatment showed increased lignin S/G ratio, but overall changes on lignin properties were milder than organosolv pretreatment. Instead of the maximum adsorption capacity increase, this pretreatment increased the adsorption affinity of lignin. Non-productive enzyme adsorption on lignin is a major lignin-derived inhibitory effect on biomass conversion. A binding strength incorporating maximum adsorption capacity and adsorption affinity served as an index of the non-productive enzyme adsorption. Specifically, maximum adsorption capacity was more affected by the contents of phenolic hydroxyl groups, while adsorption affinity showed a positive correlation with lignin S/G ratio. The results indicate that lignin-derived inhibitory effects can be diminished by lignin removal and/or alternation of physical properties of lignins. This study also provides important clues how to modify biomass for effective biomass utilization.

Experimental

Materials

The enzyme mixtures (Cellic CTec2 and HTec2) were provided by Novozymes (Franklinton, NC). Sulfuric acid and acetic anhydride were purchased from Sigma-Aldrich (St Louis, MO). Anhydrous pyridine, ethanol, ammonium hydroxide, and toluene were obtained from VWR (Suwanee, GA).

Lignin substrate preparation

Cellulolytic enzyme lignin (CEL) was isolated from Populus. The Populus samples were milled and screened to 0.42 mm using a Wiley mill (Thomas Scientific, Swedesboro, NJ), and then Soxhlet-extracted with ethanol/toluene (1 : 2, v/v) for 24 h. The extractives-free Populus was air-dried and ball-milled using Retsch PM 100 at 580 rpm for 2.5 h. Recovered ball-milled biomass was hydrolyzed at 50 °C for 48 h using the CTec2 and HTec2 enzyme mixture (140 mg protein loading per

 This journal is © The Royal Society of Chemistry 2017

Published on 05 April 2017. Downloaded by University of Tennessee at Knoxville on 05/04/2017 19:53:36.

g biomass) with 1.0 M citrate buffer solution. The enzymatic hydrolysis was repeated with fresh enzyme mixture under the same conditions for the further purification. The recovered solids were treated with protease (Protease from Streptomyces, Sigma-Aldrich) to remove residual enzymes at 37 °C for 24 h. The protease was deactivated at 100 °C for 10 min prior to freeze-drying. The recovered lignin-enriched residue was extracted by 96% dioxane at room temperature for 48 h. Dioxane-extracted lignin was recovered using a rotary evaporator and freeze-dried.

Pretreatments

Two different delignification pretreatment methods (organosolv and ammonia pretreatment) were conducted to understand the changes on lignin characteristics. The ethanol organosolv pretreatment was conduced with the CEL (~800 mg) using 60% ethanol (10 mL) containing 1.25% sulfuric acid at 180 °C for 20 min. The ammonia pretreatment was also performed with the CEL in 5% ammonium hydroxide under the same reaction temperature and time. The pretreatment was conducted using a Parr 4590 reactor (Parr Instrument Company, Moline, IL) with a Parr 4848 temperature controller (Parr Instrument Company, Moline, IL). After each pretreatment, residual solid and soluble lignin (ammonia lignin and organosolv lignin) were recovered by filtering and washing with deionized (DI) water. The solid residues and hydrolysate were freeze-dried for 72 h prior to conducting the NMR and GPC analysis. Each pretreatment was conducted in duplicates.

Chemical compositional analysis

The compositional analysis of samples was conducted as described in the NREL protocol.[46] The total lignin contents were quantified with acid soluble and acid insoluble lignins after two-step acid hydrolysis. The hydrolyzed monomeric sugar units were quantified *via* a Dionex high performance ion chromatography (HPIC) (ICS-3000, Thermo Fisher Scientific, Sunnyvale, CA) equipped with Dionex CarboPac PA20 column.

Enzyme adsorption

Cellulase adsorption on lignin samples was performed at 4 °C in 50 mM citrate buffer (pH 4.8) using cellulase C2730 (from T. reesei ATCC 26921, protein content 40 mg mL^{-1}, Sigma-Aldrich) as described previously.[47] In detail, 30 mg of each sample was added independently in a range of enzyme concentrations (0.05 to 2.0 mg mL^{-1} in citrate buffer) at 2% substrate consistency loading. Avicel was used as a control substrate for testing the enzyme adsorption. The mixture was incubated at 4 °C for 3 h at 150 rpm to reach the equilibrium. The protein content in the supernatant was determined for the free cellulase by Bradford assay using BSA as protein standard. The adsorbed cellulases were calculated by taking the difference between the initial cellulase content and the free cellulase content in the supernatant. The classical Langmuir adsorption isotherm was applied to the cellulase adsorption on lignin and Avicel in solution. In this case, the surface concentration of adsorbed enzymes (Γ) was given by the equation:

$$\Gamma = \frac{\Gamma_{max} \times C}{1/K + C}$$

where Γ_{max} is the surface concentration of protein at full coverage (mg g^{-1} substrate), K is the Langmuir constant (mL mg^{-1}), and C is the free protein concentration in the bulk solution (mg mL^{-1}). The Γ_{max} and K, representing maximum adsorption capacity and adsorption affinity, were determined from the nonlinear regression of experimental data according to the Langmuir adsorption isotherm. The binding strength, R, was calculated from Γ_{max} and K ($R = \Gamma_{max} \times K$).

Enzymatic digestibility

Enzymatic digestibility of Avicel with different lignin (CEL, OR, and AR) mixtures was tested. The CEL or each lignin residue after the pretreatments (5 and 20 mg) was loaded with Avicel (100 mg) and antibiotics (Antibiotic Antimycotic Solution, Sigma-Aldrich) in 50 mM citrate buffer solution (pH 4.8). The hydrolysis was conducted with Novozymes CTec2 (10 FPU g^{-1} glucan) at 50 °C for 72 h. To monitor the cellulose hydrolysis, 0.5 mL of supernatant in each sample was periodically taken (6, 12, 24, 48, and 72 h). The released glucose in the supernatant was quantified using a Dionex HPLC system (ICS-3000, Thermo Fisher Scientific, Sunnyvale, CA) equipped with Dionex CarboPac PA20 column.

Gel permeation chromatographic (GPC)

The weight-average molecular weight (M_w) and number-average molecular weight (M_n) of samples were measured by GPC after derivatization as previously described.[48] Briefly, the lignin and solid residues after the pretreatments were derivatized with acetic anhydride/pyridine mixture at room temperature for 24 h. The derivatized samples were dissolved in THF for GPC analysis. The molecular weights were estimated by size-exclusion separation performed on an Agilent 1200 HPLC system (Agilent Technologies, Santa Clara, CA) equipped with Waters Styragel columns (HR1, HR4, and HR5; Waters Corporation, Milford, MA).

Heteronuclear single quantum coherence (HSQC) nuclear magnetic resonance (NMR)

The lignin samples (~50 mg) were loaded with DMSO-d_6 in a 5 mm NMR tube. Two-dimensional (2D) ^{1}H–^{13}C heteronuclear single quantum coherence (HSQC) NMR experiment was conducted at 298 K using a Bruker Avance III 400 MHz spectroscopy equipped with a 5 mm Broadband Observe probe (5 mm BBO 400 MHz W1 with Z-gradient probe, Bruker). A Bruker standard pulse sequence ('hsqcetgpsi2') was applied under the following parameters: spectral width of 11 ppm in F2 (1H) with 2048 data points and 190 ppm in F1 (13C) with 256 data points; 128 scans (NS) and 1 s interscan delay (D1). Bruker's TopSpin 3.5 software was used for volume integration of contours in HSQC spectra.

Published on 05 April 2017. Downloaded by University of Tennessee at Knoxville on 05/04/2017 19:53:36.

^{31}P nuclear magnetic resonance (NMR)

For the quantification of hydroxyl groups in the lignin samples, phosphorylation of each sample was performed with 2-chloro-4,4,5,5-tetramethyl-1,3,2-dioxaphospholane (TMDP) in a solvent of pyridine/$CDCl_3$ (1.6/1.0, v/v) as described in the previous study.[49] The stock solution was prepared with pyridine/deuterated chloroform (500 μL) including 1 mg mL^{-1} $Cr(acac)_3$ and 4 mg mL^{-1} internal standard (*endo N*-hydroxy-5-norbene-2,3-dicarboxylic acid imide). About 20.0 mg of lignin sample was dissolved in the stock solution, and phosphorylation was conducted by adding 50 μL of the phosphorylating reagent TMDP. Quantitative ^{31}P NMR spectra were acquired on a Bruker Avance 400 MHz spectrometer equipped with a BBO probe using an inverse-gated decoupling pulse sequence (Waltz-16), 90° pulse, 25 s pulse delay with 64 scans. All chemical shifts reported are relative to the product of TMDP with water at 132.2 ppm.

Fourier transform infrared (FTIR)

Characterization of lignin samples was conducted with FTIR spectroscopy (Spectrum One FTIR system, PerkinElmer, Wellesley, MA) with a universal attenuated total reflection (ATR) accessory. FTIR spectra were obtained by averaging 32 scans from 4000 to 600 cm^{-1}.

Abbreviations

AL	Ammonia lignin
AR	Ammonia lignin residue
CEL	Cellulolytic enzyme lignin
FTIR	Fourier transform infrared
G	Guaiacyl
GPC	Gel permeation chromatography
HPIC	High performance ion chromatography
HSQC	Heteronuclear single quantum coherence
NMR	Nuclear magnetic resonance
LCC	Lignin-carbohydrate complexes
Mn	Number average molecular weight
Mw	Weight average molecular weight
OL	Organosolv lignin
OR	Organosolv lignin residue
PB	*p*-Hydroxybenzoate
PDI	Polydispersity index
S	Syringyl

Acknowledgements

This manuscript has been authored by UT-Battelle, LLC under Contract No. DE-AC05-00OR22725 with the U.S. Department of Energy. This study was supported and performed as part of the BioEnergy Science Center (BESC). The BioEnergy Science Center is a U.S. Department of Energy Bioenergy Research Center supported by the Office of Biological and Environmental Research in the DOE Office of Science.

Notes and references

1 R. A. Sheldon, *Green Chem.*, 2014, **16**, 950–963.
2 Z. Yu, K. S. Gwak, T. Treasure, H. Jameel, H. m. Chang and S. Park, *ChemSusChem*, 2014, **7**, 1942–1950.
3 J. L. Rahikainen, R. Martin-Sampedro, H. Heikkinen, S. Rovio, K. Marjamaa, T. Tamminen, O. J. Rojas and K. Kruus, *Bioresour. Technol.*, 2013, **133**, 270–278.
4 F. M. Medie, G. J. Davies, M. Drancourt and B. Henrissat, *Nat. Rev. Microbiol.*, 2012, **10**, 227–234.
5 X. Li and C. Chapple, *Plant Physiol.*, 2010, **154**, 449–452.
6 Y. Pu, F. Hu, F. Huang, B. H. Davison and A. J. Ragauskas, *Biotechnol. Biofuels*, 2013, **6**, 1.
7 Q. Yang and X. Pan, *Biotechnol. Bioeng.*, 2015, **113**, 1213–1224.
8 S. Nakagame, R. P. Chandra, J. F. Kadla and J. N. Saddler, *Bioresour. Technol.*, 2011, **102**, 4507–4517.
9 S. Sun, Y. Huang, R. Sun and M. Tu, *Green Chem.*, 2016, **18**, 4276–4286.
10 E. Ximenes, Y. Kim, N. Mosier, B. Dien and M. Ladisch, *Enzyme Microb. Technol.*, 2011, **48**, 54–60.
11 B.-Z. Li, V. Balan, Y.-J. Yuan and B. E. Dale, *Bioresour. Technol.*, 2010, **101**, 1285–1292.
12 X. Pan, D. Xie, R. W. Yu and J. N. Saddler, *Biotechnol. Bioeng.*, 2008, **101**, 39–48.
13 C. G. Yoo, H. Kim, F. Lu, A. Azarpira, X. Pan, K. K. Oh, J. S. Kim, J. Ralph and T. H. Kim, *BioEnergy Res.*, 2016, **9**, 67–76.
14 J. Zhu, X. Pan, G. Wang and R. Gleisner, *Bioresour. Technol.*, 2009, **100**, 2411–2418.
15 S. P. Chundawat, B. Venkatesh and B. E. Dale, *Biotechnol. Bioeng.*, 2007, **96**, 219–231.
16 S. Cao, Y. Pu, M. Studer, C. Wyman and A. J. Ragauskas, *RSC Adv.*, 2012, **2**, 10925–10936.
17 Q.-P. Liu, X.-D. Hou, N. Li and M.-H. Zong, *Green Chem.*, 2012, **14**, 304–307.
18 A. R. C. Morais, J. V. Pinto, D. Nunes, L. B. Roseiro, M. C. a. o. Oliveira, E. Fortunato and R. Bogel-Łukasik, *ACS Sustainable Chem. Eng.*, 2016, **4**, 1643–1652.
19 X. Zhao, K. Cheng and D. Liu, *Appl. Microbiol. Biotechnol.*, 2009, **82**, 815–827.
20 X. Pan, N. Gilkes, J. Kadla, K. Pye, S. Saka, D. Gregg, K. Ehara, D. Xie, D. Lam and J. Saddler, *Biotechnol. Bioeng.*, 2006, **94**, 851–861.
21 Z. Zhang, M. D. Harrison, D. W. Rackemann, W. O. Doherty and I. M. O'Hara, *Green Chem.*, 2016, **18**, 360–381.
22 H. Teramura, K. Sasaki, T. Oshima, F. Matsuda, M. Okamoto, T. Shirai, H. Kawaguchi, C. Ogino, K. Hirano and T. Sazuka, *Biotechnol. Biofuels*, 2016, **9**, 27.
23 F. F. Sun, X. Zhao, J. Hong, Y. Tang, L. Wang, H. Sun, X. Li and J. Hu, *Biotechnol. Biofuels*, 2016, **9**, 59.
24 R. Katahira, A. Mittal, K. McKinney, P. N. Ciesielski, B. S. Donohoe, S. K. Black, D. K. Johnson, M. J. Biddy and G. T. Beckham, *ACS Sustainable Chem. Eng.*, 2014, **2**, 1364–1376.

 This journal is © The Royal Society of Chemistry 2017

Published on 05 April 2017. Downloaded by University of Tennessee at Knoxville on 05/04/2017 19:53:36.

25 F. Geilen, B. Engendahl, A. Harwardt, W. Marquardt, J. Klankermayer and W. Leitner, *Angew. Chem., Int. Ed.*, 2010, **122**, 5642–5646.
26 T. Y. Nguyen, C. M. Cai, R. Kumar and C. E. Wyman, *ChemSusChem*, 2015, **8**, 1716–1725.
27 J. Luterbacher, D. M. Alonso and J. Dumesic, *Green Chem.*, 2014, **16**, 4816–4838.
28 T. H. Kim, F. Taylor and K. B. Hicks, *Bioresour. Technol.*, 2008, **99**, 5694–5702.
29 J. S. Kim, Y. Lee and T. H. Kim, *Bioresour. Technol.*, 2016, **199**, 42–48.
30 C. G. Yoo, N. P. Nghiem, K. B. Hicks and T. H. Kim, *Bioresour. Technol.*, 2011, **102**, 10028–10034.
31 F. Guo, W. Shi, W. Sun, X. Li, F. Wang, J. Zhao and Y. Qu, *Biotechnol. Biofuels*, 2014, **7**, 38.
32 N. Pareek, T. Gillgren and L. J. Jönsson, *Bioresour. Technol.*, 2013, **148**, 70–77.
33 Y. Li, Z. Sun, X. Ge and J. Zhang, *Biotechnol. Biofuels*, 2016, **9**, 20.
34 A. Guerra, I. Filpponen, L. A. Lucia and D. S. Argyropoulos, *J. Agric. Food Chem.*, 2006, **54**, 9696–9705.
35 H.-m. Chang, E. B. Cowling and W. Brown, *Holzforschung*, 1975, **29**, 153–159.
36 J. Ralph, T. Akiyama, H. D. Coleman and S. D. Mansfield, *BioEnergy Res.*, 2012, **5**, 1009–1019.
37 Y. Pu, S. Cao and A. J. Ragauskas, *Energy Environ. Sci.*, 2011, **4**, 3154–3166.
38 B. B. Hallac, Y. Pu and A. J. Ragauskas, *Energy Fuels*, 2010, **24**, 2723–2732.
39 R. Gupta and Y. Lee, *Biotechnol. Prog.*, 2009, **25**, 357–364.
40 V. Balan, L. d. C. Sousa, S. P. Chundawat, D. Marshall, L. N. Sharma, C. K. Chambliss and B. E. Dale, *Biotechnol. Prog.*, 2009, **25**, 365–375.
41 Y. Li, Z. Sun, X. Ge and J. Zhang, *Biotechnol. Biofuels*, 2016, **9**, 20.
42 X. Lu, X. Zheng, X. Li and J. Zhao, *Biotechnol. Biofuels*, 2016, **9**, 118.
43 M. Tu, X. Pan and J. N. Saddler, *J. Agric. Food Chem.*, 2009, **57**, 7771–7778.
44 O. Skyba, C. J. Douglas and S. D. Mansfield, *Appl. Environ. Microbiol.*, 2013, **79**, 2560–2571.
45 L. Qin, W.-C. Li, L. Liu, J.-Q. Zhu, X. Li, B.-Z. Li and Y.-J. Yuan, *Biotechnol. Biofuels*, 2016, **9**, 1.
46 A. Sluiter, B. Hames, R. Ruiz, C. Scarlata, J. Sluiter, D. Templeton and D. Crocker, Determination of structural carbohydrates and lignin in biomass, NREL, 2011.
47 M. Li, M. Tu, D. Cao, P. Bass and S. Adhikari, *J. Agric. Food Chem.*, 2013, **61**, 646–654.
48 R. Kumar, F. Hu, C. A. Hubbell, A. J. Ragauskas and C. E. Wyman, *Bioresour. Technol.*, 2013, **130**, 372–381.
49 A. Granata and D. S. Argyropoulos, *J. Agric. Food Chem.*, 1995, **43**, 1538–1544.